I CIMMEC
1º CONGRESSO INTERNACIONAL DE METROLOGIA MECÂNICA
DE 8 A 10 DE OUTUBRO DE 2008
Rio de janeiro, Brasil

PERFILOMETRY BY SPECKLE INTERFEROMETRY WITH MULTIMODE LASERS

Eduardo A. Barbosa, Danilo Pereira Gonçalves
Laboratório de Óptica Aplicada, Faculdade de Tecnologia de São Paulo,
CEETEPS-UNESP, Pça Cel Fernando Prestes, 30,
CEP 01124 060, São Paulo – SP, Brazil
ebarbosa@fatecsp.br

Abstract: The performance and the potencialities of profilometry by Digital Speckle Pattern Interferometry (DSPI) with diode lasers are demonstrated. The multi-wavelength character of the diode laser emission provides speckled images covered of interference fringes corresponding to the surface relief in single-exposure processes. For fringe pattern evaluation, the four-frame phase stepping technique was employed. The surface analyses of simple structures and objects like a flat metallic bar and a spherical surface were performed.

Keywords: multimode lasers, interferometry, speckle, profilometry.

1. INTRODUCTION

Interferometric methods are very useful in a wide range of metrology applications. Among them, Electronic Speckle Pattern Interferometry (ESPI) presents many interesting features like whole field analysis, real-time displaying of interference fringes through standard TV cameras and relaxed conditions for optical setup stability, if compared to other interferometric techniques. Since its development, ESPI has found several applications in displacement analysis, vibration measurement, material research and surface analysis [1] Its reliability, simplicity and applicability in noisy environments enabled the employ of ESPI for scientific and industrial purposes with the development of commercial devices.

A significant part of the current research in optical profilometry for real-life applications depends on the design and construction of optical setups with good and reliable performances in noisy environments and on faster and simpler measurement procedures. Aiming to this condition we study the use of a multimode, large free-spectral range (FSR) diode laser for surface contouring through ESPI. Due to the multi-wavelength character of the laser emission, the object image appears covered of interference contour fringes with only one diode laser in single-exposure processes. The synthetic wavelength in this case is inversely proportional to the laser FSR.

Whole-field optical interferometry using such lasers was already demonstrated in multi-wavelength holography in sillenite $Bi_{12}TiO_{20}$ crystals [2]. In that case, multiple holographic gratings were stored in the medium and the resulting diffraction efficiency was dependent on the optical path difference between the reference and the object beams, thus generating contour fringes in a single exposure. Low-coherence fiber-based ESPI using pulsed multimode diode lasers was applied for surface shaping. The coherence length of the lasers was about 150 μm and the interferogram evaluation was carried out through the five-stepping technique [3].

In this work we propose the use of a multimode, large free-spectral range (FSR) diode laser for surface contouring through DSPI (Digital Speckle Pattern Interferometry). Due to the multi-wavelength character of the laser emission, the object image appears covered of interference contour fringes with only one diode laser in single-exposure processes. The synthetic wavelength in this case is inversely proportional to the laser FSR.

The speckle pattern originated from the object illuminated by a multimode diode laser is formed on the faceplate of a CCD camera and the interferogram containing the information of the object relief is obtained without further laser tuning. Additive multi-wavelength ESPI is performed in single-exposure processes with a single multimode laser. In order to enhance the interferogram visibility, two consecutive frames in the same setup configuration were subtracted. Thus, the typical background noise from the speckle pattern was removed. The quantitative interferogram analysis was performed through phase stepping techniques. This was made by acquiring many interferogram frames and applying a discrete phase shift on the reference wave between each frame. The resulting phase map was unwrapped through the Branch-cut Method. In the experiments the performance of the method was demonstrated by measuring the relief of an flat plate and a rigid spherical surface.

2. THEORY

2.1 Contour Fringe Generation

In this section the contour fringe formation on the object surface is described. We adopted the subtractive method for interferogram visualization. Let us consider the interference of the object (S_N) and reference (R_N) waves onto a CCD target. Both waves originate from a multimode laser with

emission centered at $\bar{\lambda}$ and wavelength gap $\Delta\lambda$ between consecutive laser modes, so that S_N and R_N can be written as [1]

$$R_N = R_0 \sum_{n=-(N-1)/2}^{n=(N-1)/2} A_n \exp\left\{i[(\bar{k}+n\Delta k)\Gamma_R + \phi_n]\right\}$$
$$S_N = S_0 \sum_{n=-(N-1)/2}^{n=(N-1)/2} A_n \exp\left\{i[(\bar{k}+n\Delta k)\Gamma_S + \phi_n]\right\} \quad (1)$$

where N is the number of oscillating modes, ϕ_n is the phase of the n-th mode at the laser output, $\bar{k} \equiv 2\pi/\bar{\lambda}$, $\Delta k \equiv 2\pi\Delta\lambda/\bar{\lambda}$, A_n is a real coefficient and Γ_S and Γ_R are the optical paths of the object and the reference beams, respectively. For the first frame, the interference of both beams on the CCD is expressed by

$$I_1 = |S_N|^2 + |R_N|^2 + S_N^* R_N + R_N^* S_N \quad (2)$$

Since different modes are not mutually coherent, the following orthonormality condition must be obeyed [4]:

$$S_n^* R_m = \delta_{n,m}\, S_0 R_0 A_n A_m \times \exp\left\{-i[(\bar{k}+n\Delta k)\Gamma_S + \phi_n]\right\}\exp\left\{i[(\bar{k}+m\Delta k)\Gamma_R + \phi_m]\right\} \quad (3)$$

By applying condition (3), equation (2) yields

$$I_1 = S_0^2 + R_0^2 + S_0 R_0 \exp\left[i\bar{k}(\Gamma_S - \Gamma_R)\right]\sum_{n=-(N-1)/2}^{n=(N-1)/2} A_n^2 \exp\left[in\Delta k(\Gamma_S - \Gamma_R)\right] + R_0 S_0 \exp\left[-i\bar{k}(\Gamma_S - \Gamma_R)\right]\sum_{n=-(N-1)/2}^{n=(N-1)/2} A_n^2 \exp\left[-in\Delta k(\Gamma_S - \Gamma_R)\right] \quad (4)$$

Since the sums in the third and the fourth terms of the right-hand side of the equation above are equal, equation (4) yields

$$I_1 = S_0^2 + R_0^2 + 2R_0 S_0 \cos\left[\bar{k}(\Gamma_S - \Gamma_R)\right]\times \sum_{n=-(N-1)/2}^{n=(N-1)/2} A_n^2 \exp\left[in\Delta k(\Gamma_S - \Gamma_R)\right] \quad (5)$$

For fringe pattern visualization, the reference beam is then sinusoidally phase-modulated, and a second frame is captured and stored. This modulation can be made by attaching the mirror which delivers the reference beam to a transducer vibrating at tens of Hertz with amplitude of few μm. If the amplitude of the phase modulation is large enough, the speckle pattern is decorrelated and the intensity of the second frame is just $I_2 = S_0^2 + R_0^2$. After the subtraction of both frames and rectification, the resulting frame is given by

$$I = I_2 - I_1 = 2R_0 S_0 \times \left|\cos\left[\bar{k}(\Gamma_S - \Gamma_R)\right]\sum_{n=-(N-1)/2}^{n=(N-1)/2} A_n^2 \exp\left[in\Delta k(\Gamma_S - \Gamma_R)\right]\right| \quad (6)$$

The cos-term in the equation above represents the high spatial frequency modulation of the interference pattern and the random behavior of the speckle pattern. This term is highly sensitive to phase shifts of the order of $\bar{\lambda}$ in one of the interfering beams. Since $\bar{k} >> \Delta k$ typically, the second term has a low spatial frequency and is modulated according to the relief of the object surface, leading to interference contour fringes. The intensity in the expression above must be averaged by low-pass filtering and then squared in order to suppress the high-spatial frequency term and provide only positive values. Thus, from equation (6) one gets the interferogram signal V:

$$V \equiv < I >^2 = 2R_0 S_0 \left(\sum_{n=-(N-1)/2}^{n=(N-1)/2} A_n^2 \exp\left[in\Delta k(\Gamma_S - \Gamma_R)\right]\right)^2 \quad (7)$$

For interferogram analysis the equation above can be simplified by assuming that all modes oscillate with equal amplitudes, i.e. $A_n = 1$, so that V becomes

$$V = 2R_0 S_0 \frac{\sin^2\left[N\Delta k(\Gamma_S - \Gamma_R)/2\right]}{\sin^2\left[\Delta k(\Gamma_S - \Gamma_R)/2\right]} \quad (8)$$

From the equation above, while the phase $\Delta k[\Gamma_{S,P} - \Gamma_R]$ of a given point P on a bright fringe is

$$\Delta k(\Gamma_{S,P} - \Gamma_R) = 2\pi q\ , \quad (9)$$

the light phase from a point O laying on the next bright fringe is given by

$$\Delta k(\Gamma_{S,O} - \Gamma_R) = 2\pi(q+1)\ , \quad (10)$$

where q =1,2,... By combining the equations above one may easily determine the difference on the optical paths between points O and P (i.e., between any pair of adjacent fringes) as a function of the wavelength difference $\Delta\lambda$:

$$\Gamma_{S,O} - \Gamma_{S,P} = \frac{2\pi}{\Delta k} = \frac{\lambda^2}{\Delta\lambda} \quad (11)$$

Considering that both the beam inciding on the object surface and the beam scattered from it propagate in nearly opposite directions one gets the distance Δz between two neighboring planes of constant elevation :

$$\Delta z = \frac{\lambda^2}{2\Delta\lambda} \equiv \frac{\lambda_s}{2} \quad (12)$$

The parameter λ_S is the so-called synthetic wavelength. For a laser with a resonator length L the FSR is $\Delta\nu = c/2L$. The wavelength gap $\Delta\lambda$ in turn is related to the FSR as $\Delta\nu = c\Delta\lambda/\lambda^2$. Hence, the depth difference between two adjacent fringes is simply $\Delta z = L$, i.e., the shorter the laser cavity, the higher the spatial frequency of the fringe pattern.

2.2 Phase Stepping – The four-frame phase stepping procedure was applied for fringe evaluation. This technique is carried out by sequentially phase shifting one of the interfering beams in the optical setup by discrete phase values. Thus, from equation (8) the intensity of the $l-th$ frame at a point (x,y) can be written as [5,6]

$$V_l = \left\{ 2R_0 S_0 \frac{\sin[N_{eff}(\Delta k \Gamma_s(x,y) + l\phi)/2]}{\sin[(\Delta k \Gamma_s(x,y)/2 + l\phi)/2]} \right\}^2, \qquad (13)$$

where l is an integer and ϕ is a discrete phase shift.

The four-frame procedure is the most employed phase stepping technique for interferogram analysis. The intensities of the frames are obtained from equation (13) for $l = 0,1,2$ and 3 and for $\phi = \pi/2$ rad. Thus, one gets the well-known formula

$$\phi_{4-step} = \arctan\left(\frac{V_3 - V_1}{V_0 - V_2} \right) \qquad (14)$$

3. EXPERIMENTS

3.1 Optical Setup

The experiments were performed on the standard optical setup for DSPI shown in figure 1. The emission of the 30-mW diode laser is centered at 670 nm and its free spectral range is 53 GHz, corresponding to $\Delta\lambda$=0.082 nm. A micrometric screw supporting the mirror M3 introduces the phase shift on the reference beam. The beam splitter BS3 assures normal incidence on M3 throughout the phase stepping process. The first frame was acquired and stored, and after reference-beam phase modulation, a speckle-decorrelated second frame was obtained.

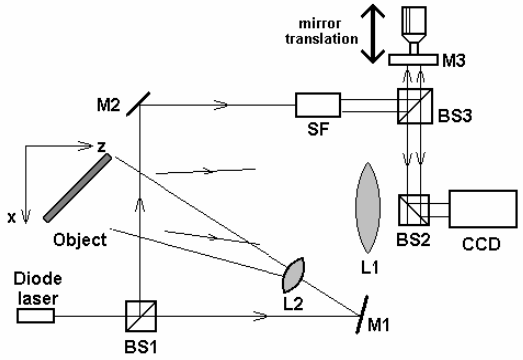

Fig. 1. Optical setup: BS1-BS3, beam splitters; L1-L3, lenses; M1-M3, mirrors; SF, spatial filter; CCD, camera

3.2 Experimental results

Figure 2a shows the multi-wavelength speckle pattern of a glass bar 20°-tilted with respect to the CCD faceplate for $\overline{\lambda} = 670$ nm with output power of 29.5 mW. Figure 2b shows the 3-D reconstruction of the tilted glass bar after applying the phase mapping and phase unwrappping processes. The measured z-coordinates (circles) of the same bar cross section reconstructed through the unwrapped phase patterns is shown in figure 2c; the solid line is the expected value of z. Figure 3 shows the (a) contour speckle interferogram and (b) the 3-D reconstruction of a spherical surface through the same procedure.

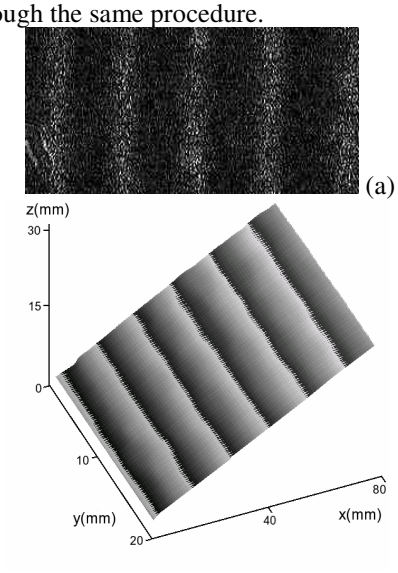

Fig. 2: profilometric analysis of a flat metallic plate

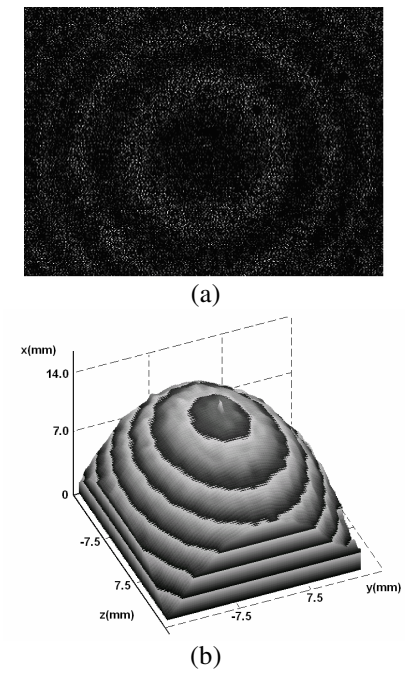

Fig. 3: profilometric analysis of a spherical object

4. CONCLUSION

We have shown that the simultaneous emission of several longitudinal laser modes does enable the generation of synthetic wavelength fringe patterns in single exposure processes and that the synthetic wavelength is half the laser resonator length. This feature make the typically short-resonator diode lasers very suitable for single exposure DSPI profilometry, thus enabling very fast, accurate and nondestructive profilometry testing. The subtractive technique was employed in order to enhance the fringe visibility. The result shows the potentialities of qualitative and quantitative nondestructive testing of surfaces with different textures and geometries, with promising applications in areas like artificial vision and quality control in agriculture and diagnosis of biological activity.

ACKNOWLEDGEMENTS

This work was supported by the Conselho Nacional de Desenvolvimento Científico (CNPq) under grant 473458/2006-3.

REFERENCES

1. R. K. Erf, *Speckle Metrology* (Academic Press, New York, 1984).

2. E. A. Barbosa, "Holographic imaging with multimode, large free spectral range lasers in photorefractive sillenite crystals", Appl. Phys. B Vol. 80, pp. 345-350, 2005.

3. P. Hariharan, B. F. Oreb, and T. Eiju, "Digital phase-shifting interferometry: a simple error-compensating phase calculation", Appl. Opt. Vol 26, pp. 2504-2505, 1987.

4. E. A. Barbosa, A. C. L. Lino, "Multi-wavelength Electronic Speckle Pattern Interferometry for Surface Shape Measurement" Appl. Opt. Vol. 46, pp. 2624-2631, 2007.

5. E. A. Barbosa, S. S. Cardoso,"Refractive and geometric lens characterization through multi-wavelength digital speckle pattern interferometry". Opt. Comm. Vol 281, pp. 1022-1029, 2008.

6. E. A. Barbosa *et al*, "Single-exposure, photorefractive holographic surface contouring with multiwavelength diode lasers" J. Opt. Soc. Am. A, Vol 22,N. 12, pp. 2872-2879, 2005.